SPIN $S=3/2$ $T_{1\rho}$ RELAXATION; THE EXCITATION OF TRIPLE-QUANTUM COHERENCES

J.R.C. VAN DER MAAREL [a], R.H. TROMP [a], J.C. LEYTE [a], J.G. HOLLANDER [a,b] and C. ERKELENS [b]

[a] *Department of Physical and Macromolecular Chemistry, Gorlaeus Laboratories, University of Leiden, P.O. Box 9502, 2300 RA Leiden, The Netherlands*

[b] *Central NMR Facility, Gorlaeus Laboratories, University of Leiden, P.O. Box 9502, 2300 RA Leiden, The Netherlands*

Received 31 January 1990

A $T_{1\rho}$ experiment on ^{23}Na in a sodium poly(methylacrylate) ion-exchange resin is reported. It is shown that due to spin $S=3/2$ $T_{1\rho}$ relaxation outside the extreme narrowing limit, triple-quantum coherences are excited. The detected line-shape of the single- as well as the triple-quantum signal contribution consists of a sum of two Lorentzians. These line-shapes and the relative intensity ratio of the single- and triple-quantum signals are in agreement with the theoretical expressions based on previously reported density-operator calculations. The spectral density at two times the precession frequency with respect to the spin-lock field is extracted from the broad component of the detected signals.

1. Introduction

The magnetic quadrupolar relaxation of spin $S=3/2$ nuclei (e.g. ^{7}Li, ^{23}Na, ^{87}Rb, ^{35}Cl, and ^{81}Br) provides information about the molecular structure and dynamics around small ions in a wide variety of condensed matter [1]. This relaxation mechanism is determined by the magnitude and temporal duration of electric-field gradients (EFG) generated by the surrounding medium [2]. Transverse and longitudinal relaxation experiments give access to the spectral density of these EFG fluctuations at zero, one, and two times the Larmor frequency with respect to the static magnetic field H_0 [3]. At the usual laboratory field strengths, this Larmor frequency is of the order of MHz. However, in the presence of slowly fluctuating processes, the spectral density may show a dispersion at relatively low frequencies of the order of kHz. Consequently, the transverse relaxation (T_2) experiment is sensitive to the zero-frequency component of this dispersion only.

One possibility to probe the spectral density in the kHz range may be to decrease the applied static magnetic field during the relaxation period. These field-cycling techniques are very fruitful in the field of proton relaxation studies [4]. However, to the authors' knowledge, for spin $S=3/2$ quadrupolar relaxation this method has found no widespread application. An alternative method may be the $T_{1\rho}$ spin-lock relaxation experiment. The $T_{1\rho}$ relaxation is sensitive to the spectral density at a frequency of the order of the precession frequency with respect to the spin-lock field H_1. The latter precession frequency is usually in the kHz range and can be varied by adapting the transmitter power.

In a previous communication, for spin $S=3/2$ a theoretical analysis of the time evolution of the density operator under spin-locking has been presented [5]. Expressions were derived which describe the resulting line shapes and relaxation rates of the detected signals. Furthermore, it was shown that outside the extreme narrowing limit triple-quantum coherences are excited. An experiment was designed to monitor these coherences. For this purpose, after the spin-lock period an additional $\pi/2$ pulse is applied. This coherence transfer pulse converts the excited triple-quantum coherences into single-quantum coherences. During the detection period, the latter coherences evolve into observable signal due to transverse relaxation.

In the present contribution, the first experimental result on spin $S=3/2$ $T_{1\rho}$ relaxation with coherence

0009-2614/90/$ 03.50

transfer ($T_{1\rho}$ CT) will be presented. The results have been obtained on a sodium poly(methylacrylate) ion-exchange resin. This resin has been selected because it is employed in more extensive research to cross-linked polyelectrolyte systems which will be published in due course [6]. This system is characterized by a high sodium capacity and hence a high signal to noise ratio. Moreover, the ^{23}Na magnetic relaxation is far outside the extreme narrowing limit but still in the Redfield regime. The detected line shapes will be analyzed using the theoretical expressions presented in previous work [5]. The derived relaxation rates are compared to the values resulting from longitudinal and transverse relaxation experiments. Especially the spectral density at two times the precession frequency with respect to the spin-lock field is compared to the spectral density at zero frequency.

2. Theory

The time-evolution of the $S=3/2$ spin system under spin-locking has been detailed in previous work and will not be repeated here. In this analysis, the density operator is expressed in terms of irreducible tensor operators. The time evolution under relaxation has been evaluated using perturbation theory [3] in a suitable interaction representation where the spin-lock field disappears. The effect of rf pulses has been calculated using the transformation properties of the irreducible tensor operators under rotation. The pulse sequence representing the $T_{1\rho}$ CT experiment is schematically depicted in fig. 1. Note the additional coherence transfer pulse after the spin-lock period.

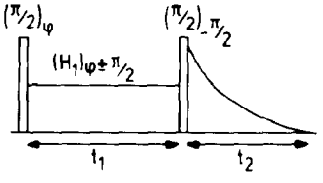

Fig. 1. $T_{1\rho}$ pulse sequence with an additional $\pi/2$ pulse after the spin-lock period. The phase φ has to be incremented proportional to the evolution time (TPPI). No power level switching between the $\pi/2$ pulses and the spin-lock pulse has been applied. The relative phase of the spin-lock field with respect to the first excitation pulse has been alternated between $\pm\pi/2$.

For ease of reference, the resulting signal contributions are summarized. In the time domain, the detected single- and triple-quantum signals are given by

$$s(t_1,t_2,p=\pm1)=[\tfrac{1}{2}f_{11}^{(\rho)}(t_1)f_{11}^{(1)}(t_2)+\tfrac{1}{32}\sqrt{6}f_{31}^{(\rho)}(t_1)f_{13}^{(1)}(t_2)]\exp(\mp i\varphi), \quad (1)$$

$$s(t_1,t_2,p=\pm3)=-\tfrac{5}{32}\sqrt{6}f_{31}^{(\rho)}(t_1)f_{13}^{(1)}(t_2)\exp(\mp 3i\varphi), \quad (2)$$

respectively, in which φ is the phase defined in fig. 1. The relaxation functions read

$$f_{11}^{(\rho)}(t)=\tfrac{1}{5}[4\exp(R_3^{(\rho)}t)+\exp(R_4^{(\rho)}t)], \quad (3)$$

$$f_{31}^{(\rho)}(t)=\tfrac{2}{5}[-\exp(R_3^{(\rho)}t)+\exp(R_4^{(\rho)}t)], \quad (4)$$

$$f_{11}^{(1)}(t)=\tfrac{1}{5}[3\exp(R_1^{(1)}t)+2\exp(R_2^{(1)}t)], \quad (5)$$

$$f_{13}^{(1)}(t)=\tfrac{1}{5}\sqrt{6}[\exp(R_1^{(1)}t)-\exp(R_2^{(1)}t)], \quad (6)$$

with rates

$$R_3^{(\rho)}=-(eQ/\hbar)^2\times[\tfrac{3}{4}J_{20}(2\omega_1)+J_{01}(\omega_0)+\tfrac{1}{4}J_{02}(2\omega_0)], \quad (7)$$

$$R_4^{(\rho)}=-(eQ/\hbar)^2[J_{01}(\omega_0)+J_{02}(2\omega_0)], \quad (8)$$

$$R_1^{(1)}=-(eQ/\hbar)^2[J_0(0)+J_1(\omega_0)], \quad (9)$$

$$R_2^{(1)}=-(eQ/\hbar)^2[J_1(\omega_0+J_2(2\omega_0)]. \quad (10)$$

The spectral densities are defined in eqs. (A.5) and (A.7) in ref. [5]. It should be noted that $J_{01}(\omega_0)$ and $J_{02}(2\omega_0)$ equal $J_1(\omega_0)$ and $J_2(2\omega_0)$, respectively, and hence $R_4^{(\rho)}=R_2^{(1)}$.

The signal has to be detected as a function of the spin-lock time t_1. The separation of coherence orders is established by time-proportional incrementation of the phase of the excitation pulse and spin-lock field: $\varphi=t_1\Delta\varphi/\Delta t_1$ (TPPI [7,8]). The signals corresponding to $\pm p$ coherences have equal amplitudes. Accordingly, after Fourier transformation with respect to the detection time t_2 (F_2 dimension), a real cosine transformation with respect to the evolution time t_1 (F_1 dimension) results in a pure 2D adsorption spectrum after suitable phase correction. The section in the F_1 dimension at the resonance position in F_2 shows two signal contributions originating from the single- and triple-quantum coherences, respectively. This frequency separation of the dif-

ferent coherence orders in the F_1 dimension has artifially been introduced by TPPI of the phase φ (see eqs. (1) and (2)).

The line shape of the single- as well as the triple-quantum signal contribution consists of a sum of two Lorentzians. The width of the broad component is determined by the relaxation rate $R_3^{(\rho)}$, whereas the width of the narrow component gives access to the rate $R_4^{(\rho)}$. According to eqs. (2) and (4), the triple-quantum signal broad and narrow components have equal amplitudes (i.e. areas) but opposite signs. For the single-quantum signal this amplitude ratio is somewhat more involved and depends on the transverse relaxation rates $R_1^{(1)}$ and $R_2^{(1)}$. The relative amplitude fractions may be calculated by expanding eq. (1) together with eqs. (3)–(6). These amplitude fractions are given by $(9+7\alpha)/(12+8\alpha)$ and $(3+\alpha)/(12+8\alpha)$ with $\alpha=R_1^{(1)}/R_2^{(1)}$ for the single-quantum signal broad and narrow components, respectively. It should be noted that these fractions apply to the section in the F_1 dimension exactly at the resonance position in F_2. For comparison, the corresponding amplitude fractions in a $T_{1\rho}$ experiment but without coherence transfer read $(3+\alpha)/(3+2\alpha)$ and $\alpha/(3+2\alpha)$, respectively. Accordingly, an additional advantage of the $T_{1\rho}$ CT experiment is the more favorable fraction of the broad component in the single-quantum signal.

3. Experimental

The poly(methylacrylate) ion-exchange resin cross-linked with 4.5% divinylbenzene (Zerolit 226) originated from BDH Chemicals Ltd, Poole. The resin was brought in the salt form by titrating with NaOH (Merck). The sodium capacity equals 5×10^{-3} mol cations per gram resin. The resin was immersed in water. The diameter of the swollen polymeric spheres is in the range 0.14×10^{-3} to 0.28×10^{-3} m. The sodium content in the surrounding water medium is negligible.

The NMR experiment was performed on a Bruker MSL 400 spectrometer equipped with a 9.4 T superconducting magnet. The resin was contained in a teflon tube to avoid spurious ^{23}Na signals originating from the sample container. A Bruker high-power probe (Z 34 v HP) equipped with a solenoid coil was used to achieve a homogeneous H_1 field. To minimize dielectric heating a Faraday shield was mounted around the sample inside the coil. This shield consisted of a set of parallel wires parallel to the H_1 field and at one side connected to ground. A high-power amplifier was tuned to achieve a H_1 field intensity of 1.5×10^{-3} T (i.e. $\omega_1=104.72\times10^3$ rad/s). The temperature was maintained at 298 ± 1 K using a gas thermostat (Bruker B-VT 1000).

The pulse sequence schematically depicted in fig. 1 was applied. To separate the different coherence orders the phase increment $\Delta\varphi$ was set to 45°. The relative phase of the spin-lock pulse and the first $\pi/2$ pulse was alternated between +90° and −90°. Finally, the whole pulse sequence as well as the receiver was subjected to an additional phase-cycling over four orthogonal phases. No power level switching between the $\pi/2$ pulses and the spin-lock pulse has been applied. The spin-lock pulse is applied exactly on resonance. A series of 512 FIDs was collected, using an evolution time increment Δt_1 of 50×10^{-6} s. Accordingly, the maximum spin-lock time equals 25.6×10^{-3} s. The 512 FIDs were Fourier transformed with respect to the detection time. The number of data points in the t_1 dimension was set to 2048 by zero filling. A real cosine Fourier transformation with respect to the evolution time and, consequently, the time-proportional phase increment results in a pure 2D absorption spectrum (after phase correction). The section in the F_1 dimension exactly at the resonance position in F_2 is presented in fig. 2.

4. Results and discussion

The separation of coherence orders has been established by TPPI of the phase φ using a phase increment of 45°. This introduces a corresponding frequency separation $\Delta\nu=\Delta\varphi/2\pi\Delta t_1$, i.e. 2.5 kHz. Accordingly, the spectrum displayed in fig. 2 discriminates between zero-, single-, double-, and triple-quantum coherences at relative frequencies: 0, 2.5, 5.0, and 7.5 kHz, respectively. The spectrum shows two different signal contributions. The feature at 2.5 kHz represents the single-quantum signal. The contribution at three times this frequency (i.e. 7.5 kHz) represents the triple-quantum signal. It is clear

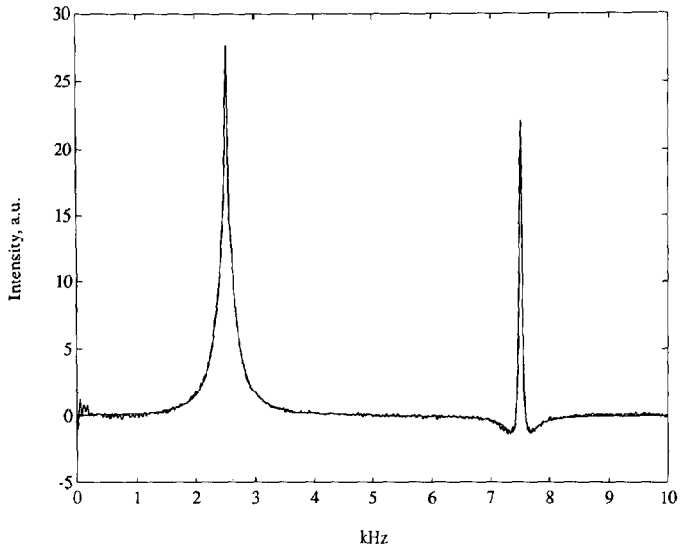

Fig. 2. ^{23}Na multiple-quantum spectrum of a sodium poly(methylacrylate) ion-exchange resin. The spectrum displays a section along the F_1 dimension at the resonance position in F_2. The feature at 2.5 kHz represents the single-quantum signal, whereas the contribution at 7.5 kHz represents the triple-quantum signal. For details see the experimental section. The solid line represents a non-linear least-squares fit of a sum of two Lorentzians to both signal contributions.

that due to $T_{1\rho}$ relaxation triple-quantum coherences are excited. Furthermore, double-quantum coherences could not be detected, which is consistent with the theoretical analysis [5].

Now the line shape of the single- as well as the triple-quantum signal contribution may be fitted to a sum of two Lorentzians. The relaxation rates and the corresponding fractions of the broad and narrow components have been estimated by a non-linear least-squares procedure [9]. The results are collected in table 1. As displayed in fig. 2, for both single- and triple-quantum coherences a sum of two Lorentzians describes the data well.

The fitted amplitude fractions corresponding to the broad and narrow components can be compared to the expected values on the basis of the density-operator calculations. As discussed in section 2, for triple-quantum coherences, the broad and narrow components have equal amplitudes but opposite signs. The fitted amplitude fractions are in reasonable agreement. For the single-quantum signal, these amplitude fractions are given by $(9+7\alpha)/(12+8\alpha)$ and $(3+\alpha)/(12+8\alpha)$ with $\alpha = R_1^{\{1\}}/R_2^{\{1\}}$. The transverse relaxation rates have been estimated using a spin-echo experiment. These relaxation rates have the values: $R_1^{\{1\}} = -1650\ \mathrm{s}^{-1}$ and $R_2^{\{1\}} = -197$

Table 1
Relaxation rates and amplitude fractions of the broad and narrow components resulting from the fit of the experimental line shapes to a sum of two Lorentzians. The derived product of the squared coupling constant and the spectral density at two times the precession frequency with respect to the spin-lock field has also been included [a]

Signal	$-R_3^{\{\rho\}}$ (s^{-1})	Fraction	$-R_4^{\{\rho\}}$ (s^{-1})	Fraction	$(eQ/\hbar)^2 J_{20}(2\omega_1)$ (s^{-1})
$s(p=\pm 1)$	1230	0.86	181	0.14	1460
$s(p=\pm 3)$	1310	−0.98	185	1.02	1560
$s(p=\pm 1)+\frac{1}{5}s(p=\pm 3)$	1220	0.81	182	0.19	1450

[a] The estimated experimental accuracy in $R_3^{\{\rho\}}$, $R_4^{\{\rho\}}$, and $(eQ/\hbar)^2 J_{20}(2\omega_1)$ is 10%.

s^{-1} (the negative sign is due to the definition of the rates, eqs. (7)–(10). Accordingly, for the single-quantum signal the theoretical amplitude fractions of the broad and narrow components equal 0.856 and 0.144, respectively. Again, the fitted fractions are in agreement with the theoretical values.

To check the relative intensities of the single- and triple-quantum signals, the triple-quantum signal may be divided by a factor five and added to the single-quantum signal. According to eqs. (1) and (2), the resulting signal reads (in the time domain)

$$s(t_1, t_2, p=\pm 1)+\tfrac{1}{5}s(t_1, t_2, p=\pm 3) = \tfrac{1}{2} f_1^{(p)}(t_1) f_1^{(1)}(t_2) . \quad (11)$$

Now, according to eq. (3), the amplitude fractions of the broad and narrow components are given by 0.80 and 0.20, respectively. Fit parameters resulting from this combination of the single- and triple-quantum signal contributions are also collected in table 1. The fitted amplitude fractions are in agreement with the theoretical values. Consequently, the relative intensities of the single- and triple-quantum signal contributions are correctly represented by eqs. (1) and (2).

After this discussion of the relative fractions of the broad and narrow components, the extracted relaxation rates will be evaluated. The relaxation rates obtained from the single- and triple-quantum signals are equal within the estimated error margin of 10%. As discussed in section 2, the relaxation rate extracted from the narrow component should equal the transverse relaxation rate $R_2^{(1)}$. The latter rate has the value $-197\ s^{-1}$, whereas the average value of $R_4^{(p)}$ equals $-183\ s^{-1}$. There is reasonable agreement.

According to eq. (7), from the experimental value of $R_4^{(p)}$ the product of the squared coupling constant and the spectral density at two times the precession frequency with respect to the spin-lock field $(eQ/\hbar)^2 J_{20}(2\omega_1)$ may be evaluated. For this purpose, the contributions $(eQ/\hbar)^2 J_1(\omega_0)$ and $(eQ/\hbar)^2 J_2(2\omega_0)$ should be known. From extensive field-dependent longitudinal and transverse relaxation experiments the latter contributions have been estimated to take the values 116 and 81 s^{-1}, respectively [6]. The resulting experimental value of the product $(eQ/\hbar)^2 J_{20}(2\omega_1)$ is also collected in table 1.

The spectral density at the frequency $2\omega_1$, (i.e. $2\omega_1 = 209.4\times 10^3$ rad/s) can be compared to the spectral density at zero frequency. The product of the squared coupling constant and $J_0(0)$ has been estimated from a spin-echo relaxation experiment: $(eQ/\hbar)^2 J_0(0) = 1530\ s^{-1}$. Within the estimated 10% error margin, this figure equals the value of $(eQ/\hbar)^2 J_{20}(2\omega_1)$ as collected in table 1. Accordingly, it can be concluded that the spectral density does not show a significant dispersion in the range $0–200\times 10^3$ rad/s.

5. Conclusions

The density-operator calculations correctly describe the relaxation behavior and time evolution of the spin $S=3/2$ system under spin-locking. It has been shown that due to $T_{1\rho}$ relaxation outside the extreme narrowing limit, triple-quantum coherences are excited. The line shapes and relative intensities are in agreement with the theoretical analysis. The relaxation rate corresponding to the narrow component compares favorably with the value obtained from transverse spin-echo experiments. The broad component provides the spectral density at two times the precession frequency with respect to the spin-lock field. In the poly(methylacrylate) ion-exchange resin the spectral density does not show a dispersion in the frequency range covered. To obtain information at higher frequencies the H_1 field strength should be increased. Unfortunately, such a transmitter power level is beyond the limits of our spectrometer technology. However, from the absence of a dispersion in the present frequency range it can be concluded that the characteristic frequencies of the electric-field gradient fluctuations exceed at least the value 30 kHz.

Acknowledgement

Dr.H. Förster is gratefully acknowledged for technical advice concerning the Faraday shield and helpful trial experiments during a stay at one of the authors at the MSL Application Laboratory, Bruker Spectrospin, Rheinstetten, FRG.

References

[1] L. van Dijk, M.L.H. Gruwel, W. Jesse, J. de Bleijser and J.C. Leyte, Biopolymers 26 (1987) 261;
C.J.M. van Rijn, J. de Bleijser and J.C. Leyte, J. Phys. Chem. 93 (1989) 5284;
S. Forsèn, T. Drakenberg and H. Wennerström, Quat. Rev. Biophys. 19 (1987) 83;
D. Petit and J.-P. Korb, Phys. Rev. B 37 (1988) 576.

[2] H. Versmold, Mol. Phys. 57 (1986) 201.

[3] A. Abragam, Principles of nuclear magnetism (Oxford Univ. Press. Oxford, 1961).

[4] S.H. Koenig and R.D. Brown III, Magn. Reson. Medicine 1 (1984) 478;
B. Borcard, Helv. Phys. Acta 60 (1987) 577;
F. Noack, M. Notter and W. Weiss, Liquid Cryst. 3 (1988) 907.

[5] J.R.C. van der Maarel, J. Chem. Phys. 91 (1989) 1446.

[6] R.H. Tromp, J.C. Leyte et al., in preparation.

[7] R.R. Ernst, G. Bodenhausen and A. Wokaun, Principles of nuclear magnetic resonance in one and two dimensions (Oxford Univ. Press, Oxford, 1987).

[8] M. Munowitz and A. Pines, Advances in chemical physics, Vol. 66, eds. I. Prigogine and S.A. Rice (Wiley, New York, 1987).

[9] A.A. Clifford, Multivariate error analysis (Applied Science Publishers, London, 1973).